Article

Neuroprotective Investigation of Chitosan Nanoparticles for Dopamine Delivery

Andrea Ragusa [1,2,]*, **Paola Priore** [2], **Anna Maria Giudetti** [3], **Giuseppe Ciccarella** [2,4] **and Antonio Gaballo** [2,]*

1   Department of Engineering for Innovation, University of Salento, via Monteroni, 73100 Lecce, Italy
2   CNR Nanotec, Institute of Nanotechnology, via Monteroni, 73100 Lecce, Italy;
    paola.priore@nanotec.cnr.it (P.P.); giuseppe.ciccarella@unisalento.it (G.C.)
3   Department of Biological and Environmental Sciences and Technologies, University of Salento,
    via Monteroni, 73100 Lecce, Italy; anna.giudetti@unisalento.it
4   Dipartimento di Scienze e Tecnologie Biologiche ed Ambientali, Università del Salento & UdR INSTM di
    Lecce, c/o Campus Ecotekne, Via Monteroni, 73100 Lecce, Italy
*   Correspondence: andrea.ragusa@unisalento.it (A.R.); antonio.gaballo@nanotec.cnr.it (A.G.)

check for
updates

Featured Application: Chitosan nanoparticles are potential candidates for the delivery of various drugs, including dopamine.

Abstract: Chitosan nanoparticles (CS NPs) have been widely exploited for the delivery of various types of drugs due to their biocompatibility, availability, ease of functionalization and other advantages. Nevertheless, despite their wide use, their mechanism of action is not very clear and many aspects still need to be investigated in detail, with only a few studies having studied the behavior of this polymer. We prepared CS NPs encapsulating dopamine (DA) and studied the generation of reactive oxygen species (ROS) and the antioxidant effect of the neurotransmitter in detail. Encapsulation of the drug and its subsequent sustained release significantly reduced the oxidation rate in vitro, thus potentially exerting neuroprotective effects. ROS production in SH-SY5Y cells was investigated through a H_2O_2 assay, while a deeper study of the enzymatic activity allowed us to determine the significant contribution of both GPx and SOD enzymes in preventing oxidative stress.

1. Introduction

Parkinson disease (PD) is a neurodegenerative disorder (ND) caused by degeneration of dopaminergic neurons in the substantia nigra [1]. Despite being the second most common neurodegenerative disease and affecting over 1% of the population above 60 years old, there is currently no cure for PD and its pharmacological therapies are based on the oral administration of DA and dopaminergic drugs to reduce the symptoms. Nevertheless, this approach has several drawbacks, such as the short half-life for circulation and rapid degradation rate, and several side effects, such as nausea, hypotension and dyskinesia. Thus, these factors reduce its therapeutic use [2,3].

Recently, nanotechnology has been shown to be able to provide valuable tools for potentially diagnosing and treating diseases in many fields of medicine, including NDs [4–10]. Furthermore, NPs can help to overcome several limitations of traditional drugs by improving their bioavailability and half-life, yielding a sustained release, in addition to allowing specific targeting [11–13]. Nanoencapsulation can also increase the stability of photosensitive molecules, enhancing their antioxidant activity only once released [14].

The exploitation of polymeric NPs in nanomedicine has several advantages due to their biocompatibility, biodegradability, ease of preparation and functionalization as well as low costs.

Chitosan is a natural polymer that has already proven to be a valuable building block for the formulation of NPs as it is able to deliver several drugs, including DA [15–17]. Furthermore, its utility in delivering drugs for treating neurological diseases has been recognized because of its ability to positively interfere in neurological processes, which occurs by chelating Cu^{2+} ions that can produce hydroxyl radicals causing lipid peroxidation [18,19].

Currently, administration of DA is the only treatment for PD. However, due to the poor efficiency of this drug in reaching the site of action, relatively high doses must be used to have a therapeutic effect. However, this leads to several undesired side-effects. Thus, to reduce the occurrence of side-effects, the delivery of DA has been attempted in various ways through nanotechnological approaches [5,15,17,20,21].

It is well known that oxidative stress plays a fundamental role in the pathophysiology of neurodegenerative diseases, such as PD. Nevertheless, to the best of our knowledge, all the articles published in the literature studied the delivery of DA from a nanotechnological point of view without investigating the mechanism of action or the effect of the drug delivery to the cells. Although the effect of free DA and free chitosan polymers have been individually investigated in detail, the same approach from a nanotechnological point of view is still missing.

In this research article, we studied the neuroprotective effect of CS NPs in vitro on SH-SY5Y cells and we investigated the different influences of the polymeric NPs, the DA and the loaded nanoformulation in generating ROS and their effect from an enzymatic point of view.

2. Materials and Methods

The following chemicals were obtained from commercial sources and used as received. Chitosan (medium molecular weight, 75–85% deacetylated, #448877), pentasodium tripolyphosphate hexahydrate (TPP, #T5633), dopamine hydrochloride (#H8502), and 3-(4,5-dimethyl-2-thiazolyl)-2,5-diphenyl-2*H*-tetrazolium bromide (MTT salt, #135038) were purchased from Sigma-Aldrich (Milan, Italy). Ultra-pure grade water with a conductivity of 18.2 MΩ cm was used in all experiments.

All the manipulations involving DA were carried out under light protection using vessels covered with aluminum foil.

2.1. Synthesis of the Nanoparticles

The synthesis of DA-loaded chitosan nanoparticles (CS(DA) NPs) was carried out based on slight modifications of previously published procedures [15,17]. Briefly, a 0.2% *w/v* solution of chitosan (3 mg) in 0.1% *v/v* AcOH/H_2O (1.5 mL) was prepared. After complete dissolution of the polymer, DA (7.5 mg) was added to the solution to reach a final 0.5% *w/v* concentration. A 0.07% *w/v* aqueous solution (1.6 mL) of TPP (1.1 mg) was added and the mixture was gently stirred. After 15 min, the formed suspension was precipitated by centrifugation and washed 3 times with deionized water at $400 \times g$ for 15 min. The resulting CS NPs were resuspended in 1 mL of ultrapure water by manual shaking, before being characterized or directly utilized for the biological experiments. The same procedure was utilized for the preparation of the CS NPs, except the DA was not added into the polymer solution.

2.2. Characterization of the Nanoparticles

Transmission elemental microscopy (TEM) analysis. Samples were prepared by dropping a solution of NPs diluted in water on carbon-coated copper grids (Formvar/Carbon 300 Mesh Cu). TEM images were recorded on a JEOL JEM-1400Plus microscope (JEOL Ltd., Tokyo, Japan) operating at an accelerating voltage of 80 kV.

DLS analysis. A Zetasizer Nano ZS90 (Malvern Instruments, Malvern, Worcestershire, UK) equipped with a 4.0-mW He-Ne laser operating at 633 nm, while an Avalanche photodiode detector was used. Measurements were made at 25 °C in phosphate-buffered saline (PBS) solutions (pH of 7.4) of the particles. The size distributions are by volume (%), while the ζ-potential measurements are by intensity. Each sample has been measured 5 times and the results were analyzed by Malvern Instruments Ltd. software.

UV–vis analysis. Spectra were recorded using a Varian Cary 300 UV–vis spectrophotometer (Varian Inc., Palo Alto, CA, USA). A calibration curve was prepared by recording DA spectra in solutions with increasing concentrations from 0.1, 0.25, 0.5, 0.75 and 1.0 mg/mL. The values of absorbance at 280 nm were recorded and plotted against the known DA concentrations. The data points were fitted with a linear regression of the intercept equal to zero, before unknown concentrations of DA were calculated by inserting the measured DA absorbance of the unknown sample into the corresponding equation.

DA loading into the NPs. The DA loading of freshly prepared CS NPs was derived indirectly by measuring the DA concentration in the solution after the synthesis. The DA in the NPs was isolated from the DA in solution by centrifugation ($16,000\times g$, 30 min). The absorbance of the free DA in solution was measured and the corresponding amount calculated from the equation of the previously prepared calibration curve. The calculated value was subtracted from the total amount of DA added to the solution during the synthesis of the NPs. The DA loading efficiency was calculated from the following equation:

$$\% \text{ DA loading} = 100 \times (\text{total DA} - \text{free DA})/\text{total DA} \tag{1}$$

In vitro release study. The release of DA from freshly prepared CS NPs was indirectly calculated in vitro at 37 °C in phosphate-buffered saline (PBS) solutions at pH values of 7.4 and 5.5 by measuring the DA concentration in the solution at prefixed time lapses of 1, 2, 3, 4, 6, 8, 18, 24 and 48 h. The concentration of the DA in solution was calculated by UV–vis analysis, as previously reported. The percentage of DA released was calculated from the following equation:

$$\% \text{ DA released} = 100 \times (\text{loaded DA} - \text{free DA})/\text{loaded DA} \tag{2}$$

Each experiment was performed in triplicate to calculate the reported standard deviations.

2.3. Biological Studies

Incubation cell conditions. Human neuroblastoma SH-SY5Y cells were grown at 37 °C in a humidified incubator with 5% CO_2 in Dulbecco's modified Eagle's medium (DMEM)-F12 medium, which was supplemented with 10% newborn calf serum, 100 Units/mL penicillin and 100 mg/mL streptomycin.

MTT test on SH-SY5Y cell line. An MTT assay was used to determine the cell viability in different conditions. For this, cells were cultured in high-glucose DMEM supplemented with 10% fetal bovine serum (FBS), 2 mM L-glutamine, 100 U/mL penicillin and 100 mg/mL streptomycin in a humidified atmosphere of 5% CO_2 at 37 °C. These were plated at 5×10^3 cells per well in a 96-well plate. After treatment, the culture medium was aspirated, before 100 mL of RPMI-phenol free medium containing 10 mL of MTT stock solution and 5 mg/mL of PBS solution was added to each well. After one hour of incubation, the MTT solution was removed and 100 mL of DMSO was added to dissolve MTT–formazan crystals. The absorbance of the converted dye was measured at a wavelength of 570 nm using an iMark microplate reader (Bio-Rad, Hercules, CA, USA). The relative cell viability was expressed as a percentage of the untreated control group.

Determination of intracellular reactive oxygen species (ROS). Hydrogen peroxide (H_2O_2) was measured by Amplex® Red Hydrogen Peroxide/Peroxidase Assay Kit (TermoFisher Scientific,

Waltham, MA, USA). The oxidation product of 1:1 stoichiometric reaction between Amplex® Red reagent and H_2O_2 was spectrophotometrically measured at 571 nm.

Glutathione peroxidase activity assay. The glutathione peroxidase (GPx) assay was performed on control cells and on cells incubated with 100 µM DA, 100 µM CS(DA) NPs and the equivalent amount of CS NPs for 24 h following the instructions reported in Cayman's GPx assay kit (Kayman Chemical, Ann Arbor, MI, USA). The activity was measured indirectly by a coupled reaction with glutathione reductase. Oxidized glutathione (GSSG) produced upon reduction of hydroperoxide by GPx is recycled to its reduced state by glutathione reductase (GR) and nicotinamide adenine dinucleotide phosphate (NADPH). The change in absorbance at 340 nm was monitored for 3 min. A blank with all ingredients except the sample was also monitored. Specific activity was calculated as U/mg protein.

Superoxide dismutase activity assay. An enzymatic assay was performed on control cells and on cells incubated with 100 µM DA, 100 µM CS(DA) NPs and the equivalent amount of CS NPs for 24 h. Superoxide Dismutase (SOD) activity was assayed with Cayman's assay kit, which utilized a tetrazolium salt for detection of superoxide radicals generated by xanthine oxidase and hypoxanthine. SOD activity was calculated using the equation obtained from the linear regression of a standard curve built in the same experimental conditions.

Statistical analysis. The analytical data were expressed as mean ± standard deviation. Statistical analysis was conducted using Student's *t*-test or one-way analysis of variance (ANOVA). Levels of statistical significance were set at $p < 0.05$, 0.005 and 0.001, as stated in the text.

3. Results

3.1. Preparation and Characterization of the NPs

The preparation of the chitosan NPs was accomplished using the gelation method with TPP as the chelating agent according to previously reported procedures [16,22]. Briefly, the CS NPs were prepared by dissolving the desired amount of DA (5 mg/mL) in the starting chitosan solution, before TPP was added in order to allow the encapsulation of the antioxidant. Thus, we finally obtained CS(DA) NPs. Bare CS NPs were also prepared and used as control in the experiments with cells.

The shape and the morphology of the CS(DA) NPs were observed by transmission electron microscopy (TEM; Figure 1). The images revealed that all NPs were quite spherical and uniform in shape. The observed mean diameter was about 80 nm for all the formulations, although some variability was clearly visible with sizes in the range of 50–100 nm. No aggregation could be observed among the NPs.
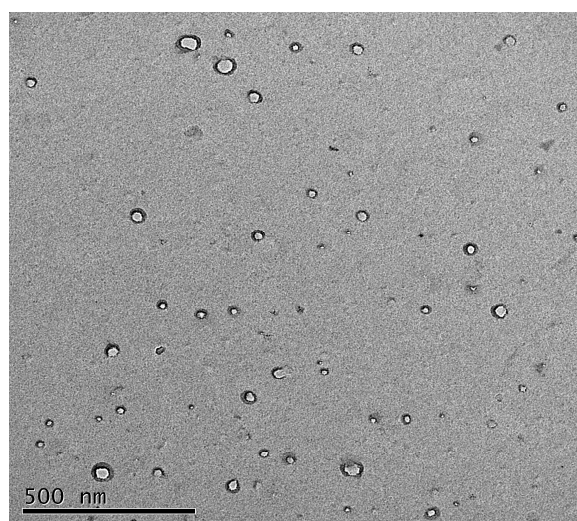

Figure 1. TEM image of CS(DA) NPs.

The hydrodynamic diameter in the PBS solution (pH of 7.4) and the corresponding polydispersity index (PDI) of the NPs were observed by DLS and the results are reported in Table 1. The formulations showed an average diameter of about 100 and 109 nm for the CS and the CS(DA) NPs, respectively. As expected, the measured size in the solution was slightly higher compared to that observed by TEM.

Table 1. Physico-chemical properties of the CS and CS(DA) NPs in PBS solution.

Sample	DA Conc. (mg/mL)	Size (nm)	PDI	ζ-Potential (mV)	DA Loading Efficiency (%)
CS NPs	0	100 ± 18	0.3	$+27 \pm 0.4$	-
CS(DA) NPs	5	109 ± 16	0.4	$+34 \pm 0.9$	64%

The observed charge of the NPs in solution was approximately 27 and 34 mV for the CS and CS(DA) NPs, respectively (Table 1). These positive values are consistent with previously reported values in the literature and are due to the free amino groups exposed to the outer environment. As expected, a bigger size of NPs results in a larger positive net charge.

The DA loading was indirectly calculated by measuring the absorbance of the starting solution used during the synthesis and the absorbance of the same solution after the gelation process. The observed DA concentration in the solution was subtracted from the starting concentration and the resulting value was assumed to be the amount of DA encapsulated into the NPs. An average encapsulation efficiency of 64% was observed over five syntheses, although this value was quite variable with the efficiency in the range of 45–75%. Furthermore, we were not able to gain perfect control over this parameter. In order to reduce variability in the subsequent experiments, two stock solutions of several milliliters each were prepared for the CS and CS(DA) NPs and these were used in all the subsequent characterization and cellular experiments.

To better understand the neuroprotective effect exerted by the CS(DA) NPs, the drug release was investigated in vitro by mimicking the environmental conditions encountered in the cellular experiments. Two physiological conditions were investigated by means of PBS solutions. The first one was conducted at a pH of 7.4, which is similar to the environment found in the cellular medium. The second one was conducted at a pH of 5.5, mimicking the intracellular endosome and lysosome ambient pH encountered after internalization of the NPs [23]. In both conditions, most of the DA release was obtained in the first few hours, with saturation almost reached after approximately 24 h (Figure 2).

The measured concentration of released DA in solution at a pH of 7.4 reached almost 50% of the initial encapsulated concentration after 48 h. As expected, the acidic conditions allowed a slightly faster DA release compared to that observed at an almost neutral pH, while the percentage of drug released was also slightly higher after 2 days. This was probably due to the protonation of the amine groups at the acidic pH, which allowed a double effect. On one hand, the electrostatic repulsion among the positively charged amines of the chitosan induced swelling of the NPs. On the other hand, the electrostatic repulsion between the amine groups of the chitosan and that of the DA allowed slightly more efficient total release of the drug after 48 h.
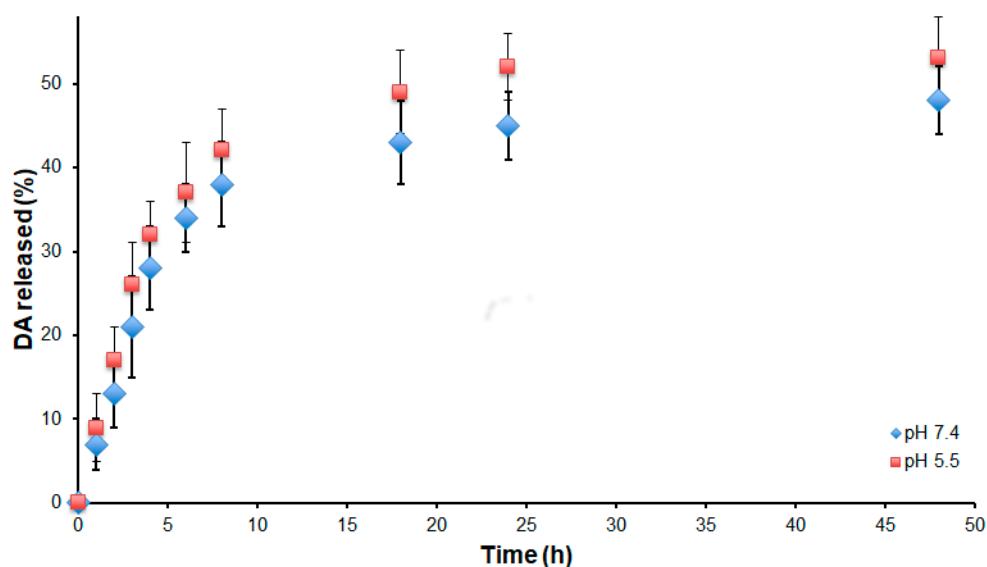
Figure 2. In vitro DA release profiles from CS(DA) NPs in PBS solutions at a pH of 7.4 (blue dots) and a pH of 5.5 (orange dots) at 37 °C. Error bars represent the standard deviation values calculated from three independent experiments.

3.2. ROS Neuroprotection by CS(DA) NPs and Enzymatic Activities

It is reported that when DA exists outside of synaptic vesicles at high concentrations, it can induce oxidative stress in cells [24,25]. This is because free DA is an unstable molecule that can oxidize spontaneously to form ROS, free radicals and quinones. For this reason, synaptic vesicles play a critical role in storing and thus, preventing DA oxidation in dopaminergic neurons. Moreover, DA is also easily metabolized by monoamine oxidase (MAO) to 3,4-dihydroxyphenylacetic acid with the concomitant formation of hydrogen peroxide [24].

DA or CS(DA) NPs were co-cultured with dopaminergic SH-SY5Y cells at suitable 5% CO_2-humidified atmosphere for 24 h. The percentage of cell viability was first evaluated by optical microscopy, before being evaluated by an MTT assay. We performed a dose dependent (25–100 μM) study for both free DA and CS(DA) NPs. The effects observed in cells treated with CS(DA) NPs were compared with those obtained from both CS NPs treated and control cells (treated with vehicle alone). In viable cells, MTT is cleaved by mitochondrial dehydrogenase to produce a purple product, which has a concentration (measured in terms of absorbance) that is directly proportional to the number of viable cells and is inversely proportional to the degree of cytotoxicity.

The addition of free DA (25–100 μM) to cells cultured in the DMEM-F12 medium showed no obvious toxicity with respect to control cells, which was demonstrated by both optical microscopy and MTT analysis (Figure 3). On the other hand, the partial loss of cell viability was induced by CS(DA) NPs at all the investigated concentrations, with respect to both control and NPs alone. However, the cell viability was always above 75% (Figure 3b). A further increase in the concentration of free DA caused more significant cellular death, which was up to 70% with 250 μM of free DA (data not shown). This is why we decided to investigate a significantly milder concentration range up to 100 μM, thus resembling more normal physiological conditions of the cellular environment.
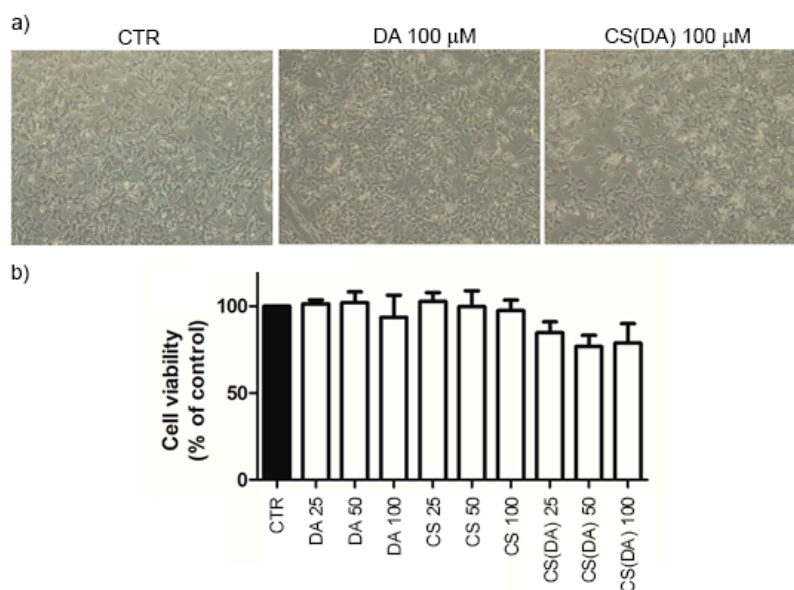
Figure 3. Dose-dependent effects of free DA and CS(DA) NPs on SH-SY5Y cell-viability. (**a**) Optical microscopy imaging of control cells (CTR), cells incubated with free DA (100 μM) and cells incubated with CS NPs loaded with the same amount of DA. (**b**) Histogram of cell viability after treatment with free DA, CS and CS(DA) NPs with respect to untreated control cells at 25, 50 and 100 μM DA concentration.

In order to obtain a better understanding of the neuroprotective effect exerted by the chitosan polymer over the delivery of free DA, we decided to inspect the generation of oxygen radicals in different conditions, which involves namely using polymeric chitosan NPs, free DA and CS(DA) NPs. As already stated, we chose to treat cells with free DA at a maximum concentration of 100 μM to simulate a condition in which cells are not affected by external DA administration and are supposed to exert their normal physiological activity.

Incubation of cells with free DA and CS(DA) NPs for 24 h caused a significant increase ($p < 0.001$) in oxidative stress with respect to the control at 100 μM concentration, which was indicated by increased H_2O_2 production (Figure 4). It is worth noting that the addition of CS NPs at the same polymeric concentration used with 100 μM CS(DA) NPs did not cause any significant toxicity to the cells (Figure 3b). However, oxidative stress in cells treated with CS(DA) NPs at the same concentration was significantly lower with respect to the values measured in cells treated with DA alone. This is probably due to the sustained release of DA over time, which is exerted by the nanoparticles, compared to the addition of 100 μM free DA in one single injection.

Intracellular mechanisms of protection from oxidative free radical damage include scavenging enzyme systems, which reduce the amount of ROS, such as superoxide dismutase (SOD) and glutathione peroxidase (GPx). Thus, we focused our attention on these enzymes to obtain a better understanding of how H_2O_2 was produced after DA addition and how this process was controlled by these scavenging enzymes.

Increased H_2O_2 production was indeed accompanied by a significant increase in the enzymatic activity of both GPx ($p < 0.001$) and SOD ($p < 0.05$) in cells treated with free DA when compared to control cells (Figure 5).
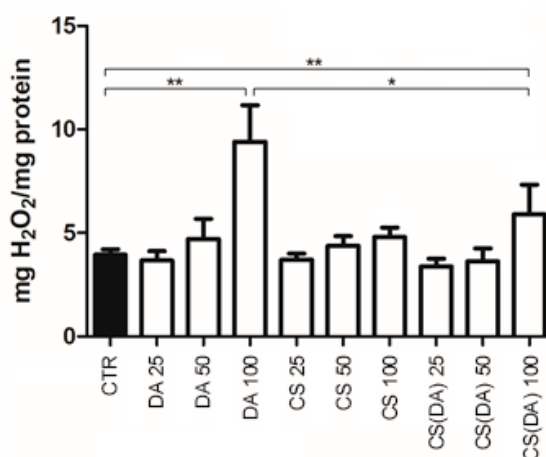
Figure 4. Amount of hydrogen peroxide produced by different incubated SH-SY5Y cell lines. Asterisks indicate statistical differences between the selected data series (* $p < 0.05$; ** $p < 0.005$).

A similar behavior was observed when the DA was delivered through the CS NPs ($p < 0.001$ and $p < 0.005$ for the GPx and SOD activity with respect to control cells, respectively). On the other hand, a statistical difference ($p < 0.001$) in the activity induced by the free and the encapsulated DA was noted only in the GPx enzyme, where the CS(DA) NPs stimulated a greater effect with respect to the free drug (Figure 5a). Although similar behavior was observed when checking the SOD enzymatic activity, no statistical significance was noted between the two delivery systems, which were namely the free and encapsulated drugs (Figure 5b). As expected, the bare CS NPs did not induce any activity in the studied enzymes with respect to the control cells. The observed increased enzymatic activity with the CS(DA) NPs compared to the free DA might be due to the sustained release exerted by the NPs. Furthermore, the NPs could protect the DA from the external environment before its release, while the free drug might be partially oxidized and become inactive in the cell media over the 24-h time experiment. This data might indicate a direct involvement of GPx and SOD in the protective effect of CS NPs against DA-induced oxidative stress. Thus, it is conceivable that the controlled release of DA from CS NPs led to an increase in the enzymatic activity, thus preventing an excessive increase in the H_2O_2 level.
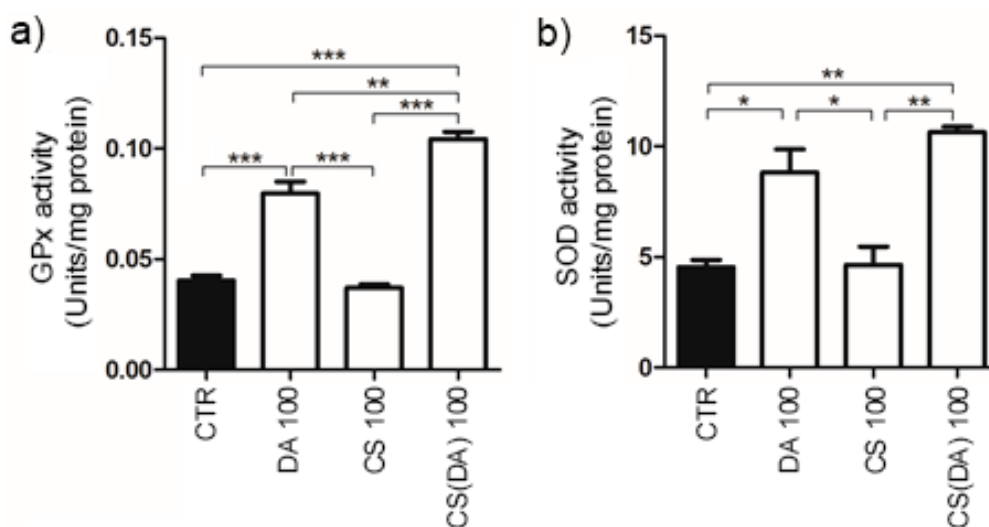

Figure 5. (**a**) GPx and (**b**) SOD antioxidant enzyme activity in control and SH-SY5Y cells treated with 100 µM DA, CS NPs and CS(DA) NPs. Asterisks indicate statistical differences between the selected data series (* $p < 0.05$; ** $p < 0.005$; *** $p < 0.001$).

4. Conclusions

Chitosan NPs have been widely employed for the delivery of various water-soluble drugs and also DA, which has been used for the treatment of neurodegenerative diseases. PD is a neurological disorder that affects over 1% of the population above 60 years old. The administration of DA is the major current treatment employed to reduce the symptoms of the pathology, although it also causes several side effects. The use of nanoformulations might reduce this inconvenience through a more efficient delivery of the neurotransmitter and a more sustained release over time. In this article, we investigated the ROS production and the enzymatic activity induced by CS(DA) NPs in SH-SY5Y cells in detail. We observed that at 100 μM concentration, the encapsulated DA induced lower H_2O_2 production compared to the free drug. This is probably due to the slower release and the protective effect exerted by the NPs, which reduces DA oxidation in cell media. An enzymatic investigation at the same concentration showed that both GPx and SOD behave quite similarly and an increase in their activity was induced by both DA and CS(DA) NPs, with the latter being relatively higher.

Our study demonstrated that the sustained release of the drug significantly reduces the oxidative stress in the cells, although the NPs also induced some toxicity. Furthermore, both GPx and SOD enzymes play a significant role in scavenging the generated ROS, thus potentially having a neuroprotective effect.

Author Contributions: A.R. conceived and designed the experiments; A.R., P.P. and A.M.G. performed the experiments; A.R., A.M.G. and A.G. analyzed the data; G.C. contributed reagents/materials; A.R., A.M.G, G.C. and A.G. wrote and revised the paper.

Conflicts of Interest: The authors declare no conflict of interest.

References

1. Schapira, A.H. Causes of neuronal death in Parkinson's disease. *Adv. Neurol.* **2001**, *86*, 155–162. [PubMed]
2. Begley, D.J. Delivery of therapeutic agents to the central nervous system: The problems and the possibilities. *Pharmacol. Ther.* **2004**, *104*, 29–45. [CrossRef] [PubMed]
3. Garbayo, E.; Ansorena, E.; Blanco-Prieto, M.J. Drug development in Parkinson's disease: From emerging molecules to innovative drug delivery systems. *Maturitas* **2013**, *76*, 272–278. [CrossRef] [PubMed]
4. Eaton, P.; Ragusa, A.; Clavel, C.; Rojas, C.T.; Graham, P.; Durán, R.V.; Penadés, S. Glyconanoparticle-DNA interactions: An atomic force microscopy study. *IEEE Trans. Nanobiosci.* **2007**, *6*, 309–318. [CrossRef]
5. Malvindi, M.A.; Di Corato, R.; Curcio, A.; Melisi, D.; Rimoli, M.G.; Tortiglione, C.; Tino, A.; George, C.; Brunetti, V.; Cingolani, R.; et al. Multiple Functionalization of Fluorescent Nanoparticles for Specific Biolabeling and Drug Delivery of Dopamine. *Nanoscale* **2011**, *3*, 5110–5119. [CrossRef] [PubMed]
6. Chiriacò, F.; Conversano, F.; Soloperto, G.; Casciaro, E.; Ragusa, A.; Sbenaglia, E.A.; Dipaola, L.; Casciaro, S. Epithelial cell biocompatibility of silica nanospheres for contrast-enhanced ultrasound molecular imaging. *J. Nanopart. Res.* **2013**, *15*. [CrossRef]
7. Conversano, F.; Soloperto, G.; Greco, A.; Ragusa, A.; Casciaro, E.; Chiriacò, F.; Demitri, C.; Gigli, G.; Maffezzoli, A.; Casciaro, S. Echographic detectability of optoacoustic signals from low-concentration PEG-coated gold nanorods. *Int. J. Nanomed.* **2012**, *7*, 4373–4389. [CrossRef]
8. Ragusa, A.; Garcia, I.; Penades, S.; García, I.; Penadés, S.; Garcia, I.; Penades, S. Nanoparticles as nonviral gene delivery vectors. *IEEE Trans. Nanobiosci.* **2007**, *6*, 319–330. [CrossRef]
9. Malvindi, M.A.; Greco, A.; Conversano, F.; Figuerola, A.; Corti, M.; Bonora, M.; Lascialfari, A.; Doumari, H.A.; Moscardini, M.; Cingolani, R.; et al. Magnetic/silica nanocomposites as dual-mode contrast agents for combined magnetic resonance imaging and ultrasonography. *Adv. Funct. Mater.* **2011**, *21*, 2548–2555. [CrossRef]
10. Re, F.; Gregori, M.; Masserini, M. Nanotechnology for neurodegenerative disorders. *Maturitas* **2012**, *73*, 45–51. [CrossRef] [PubMed]

11. Quarta, A.; Ragusa, A.; Deka, S.; Toitiglione, C.; Tino, A.; Cingolani, R.; Pellegrino, T. Bioconjugation of rod-shaped fluorescent nanocrystals for efficient targeted cell labeling. *Langmuir* **2009**. [CrossRef] [PubMed]

12. Di Corato, R.; Quarta, A.; Piacenza, P.; Ragusa, A.; Figuerola, A.; Buonsanti, R.; Cingolani, R.; Manna, L.; Pellegrino, T. Water solubilization of hydrophobic nanocrystals by means of poly(maleic anhydride-alt-1-octadecene). *J. Mater. Chem.* **2008**, *18*, 1991. [CrossRef]

13. Di Corato, R.; Bigall, N.C.; Ragusa, A.; Dorfs, D.; Genovese, A.; Marotta, R.; Manna, L.; Pellegrino, T. Multifunctional Nanobeads Based on Quantum Dots and Magnetic Nanoparticles – Synthesis and Cancer Cell Targeting and Sorting. *ACS Nano* **2011**, *5*, 1109–1121. [CrossRef] [PubMed]

14. Coradini, K.; Lima, F.O.O.; Oliveira, C.M.M.; Chaves, P.S.S.; Athayde, M.L.L.; Carvalho, L.M.M.; Beck, R.C.R. Co-encapsulation of resveratrol and curcumin in lipid-core nanocapsules improves their in vitro antioxidant effects. *Eur. J. Pharm. Biopharm.* **2014**, *88*, 178–185. [CrossRef] [PubMed]

15. Trapani, A.; De Giglio, E.; Cafagna, D.; Denora, N.; Agrimi, G.; Cassano, T.; Gaetani, S.; Cuomo, V.; Trapani, G. Characterization and evaluation of chitosan nanoparticles for dopamine brain delivery. *Int. J. Pharm.* **2011**, *419*, 296–307. [CrossRef] [PubMed]

16. De Giglio, E.; Trapani, A.; Cafagna, D.; Sabbatini, L.; Cometa, S. Dopamine-loaded chitosan nanoparticles: Formulation and analytical characterization. *Anal. Bioanal. Chem.* **2011**, *400*, 1997–2002. [CrossRef] [PubMed]

17. Di Gioia, S.; Trapani, A.; Mandracchia, D.; De Giglio, E.; Cometa, S.; Mangini, V.; Arnesano, F.; Belgiovine, G.; Castellani, S.; Pace, L.; et al. Intranasal delivery of dopamine to the striatum using glycol chitosan/sulfobutylether-??-cyclodextrin based nanoparticles. *Eur. J. Pharm. Biopharm.* **2015**, *94*, 180–193. [CrossRef] [PubMed]

18. Hao, C.; Wang, W.; Wang, S.; Zhang, L.; Guo, Y. An overview of the protective effects of chitosan and acetylated chitosan oligosaccharides against neuronal disorders. *Mar. Drugs* **2017**, *15*, 89. [CrossRef] [PubMed]

19. Queiroz, M.F.; Melo, K.R.T.; Sabry, D.A.; Sassaki, G.L.; Rocha, H.A.O. Does the use of chitosan contribute to oxalate kidney stone formation? *Mar. Drugs* **2015**, *13*, 141–158. [CrossRef] [PubMed]

20. Pahuja, R.; Seth, K.; Shukla, A.; Shukla, R.K.; Bhatnagar, P.; Chauhan, L.K.S.; Saxena, P.N.; Arun, J.; Chaudhari, B.P.; Patel, D.K.; et al. Trans-blood brain barrier delivery of dopamine-loaded nanoparticles reverses functional deficits in parkinsonian rats. *ACS Nano* **2015**, *9*, 4850–4871. [CrossRef] [PubMed]

21. Hawthorne, G.H.; Bernuci, M.P.; Bortolanza, M.; Tumas, V.; Issy, A.C.; Del-Bel, E. Nanomedicine to Overcome Current Parkinson's Treatment Liabilities: A Systematic Review. *Neurotox. Res.* **2016**, *30*, 715–729. [CrossRef] [PubMed]

22. Mao, S.; Sun, W.; Kissel, T. Chitosan-based formulations for delivery of DNA and siRNA. *Adv. Drug Deliv. Rev.* **2010**, *62*, 12–27. [CrossRef] [PubMed]

23. Schmaljohann, D. Thermo- and pH-responsive polymers in drug delivery. *Adv. Drug Deliv. Rev.* **2006**, *58*, 1655–1670. [CrossRef] [PubMed]

24. Muñoz, P.; Huenchuguala, S.; Paris, I.; Segura-Aguilar, J. Dopamine oxidation and autophagy. *Parkinsons. Dis.* **2012**, *2012*, 1–13. [CrossRef] [PubMed]

25. Zhou, Z.D.; Selvaratnam, T.; Chao, Y.X.; Lim, T.M.; Tan, E.K. Dopamine (DA) Dependent Toxicity Relevant to DA Neuron Degeneration in Parkinson's Disease (PD). *Austin J. Drug Abus. Addict.* **2016**, *3*, 1–9.